

Supersaturation between Airborne Observations

in DC3 Campaign and WRF Simulations

John J. D'Alessandro¹, Dr. Minghui Diao¹, Dr. Ming Chen²

1. Department of Meteorology and Climate Science: San Jose State University, San Jose, CA
2. National Center for Atmospheric Research, Boulder, CO

Introduction:

Anvil cirrus clouds (cumulonimbus incus) are associated with strong convection and are commonly composed entirely of ice crystals (i.e. ice clouds). They are often observed in the Tropics and the Midlatitudes.

Primary factors in convective cirrus forcings^(c):

1. Relative Humidity of ice phase (RHI)
2. Vertical Velocity
3. Existing ice particles

Relative humidity is a function of both water vapor and temperature, and is important to understand as the formation of (ice) clouds requires conditions when RHI is greater than 100% (ice supersaturation, ISS). Thus, the “birth-place” of ice clouds may be wherever Ice Supersaturated Regions (ISSRs) exist. Updraft magnitudes (vertical velocity) can impact the local cooling rate due to adiabatic expansion. This impacts droplet growth rates, homogeneously formed ice crystal concentrations, and RHI. Saturation vapor pressure can be shown to be primarily a function of temperature^(e), thus vertical velocity is an important parameter to study as it is directly related to RHI.



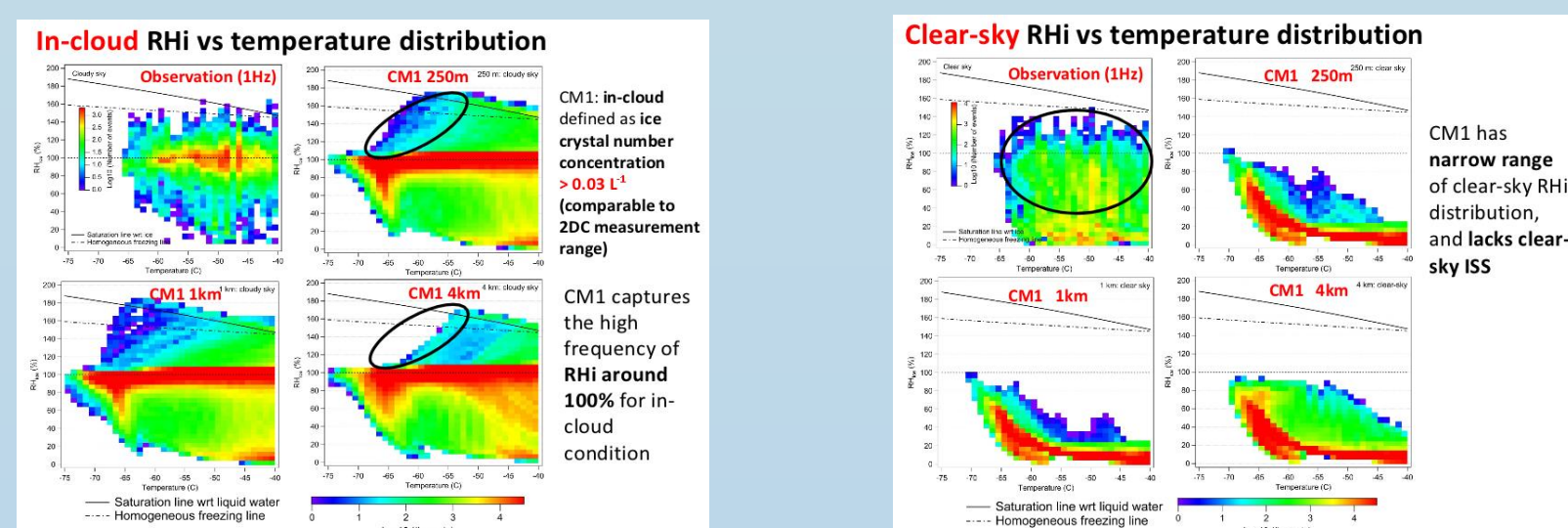
Scientific Questions:

- What occurrence frequencies of ISS are observed in anvil cirrus clouds and in surrounding clear skies?
- How does vertical velocity impact ISS formation and/or the maintenance of ISS inside anvils?
- Are stronger updrafts required for high ice supersaturation to exist?
- How do numerical weather models represent these conditions? And how well?

Importance: ISSRs and ice clouds are intimately tied to the global climate system due to their radiative properties. Improvements in understanding ice cloud formation will lead to better parameterizations for improved global and regional climate modelling.

Background:

Diao et al. (in preparation) compared flight observations of convective cirrus from the Deep Convective Cloud & Chemistry campaign (DC3) with those simulated in the NCAR Cloud Model version 1 (CM1) for an idealized squall line scenario. The CM1 captured high occurrence frequencies around 100% RHI for in-cloud conditions. However, CM1 failed to capture Ice supersaturated regions (ISSRs) for clear sky conditions (shown below^(a)):

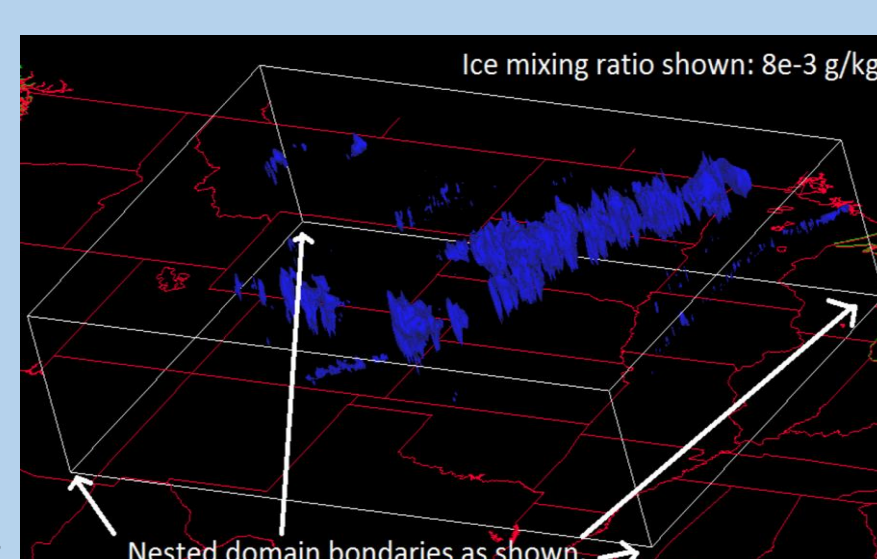


Complimentary model comparisons examining convective cirrus in the Weather Research and Forecasting model (WRF:ARW) allows for further investigation of the ability of numerical weather models to accurately represent both ISSRs and convective cirrus. Unlike CM1, WRF accounts for interactions from synoptic and mesoscale phenomenon.



Methodology:

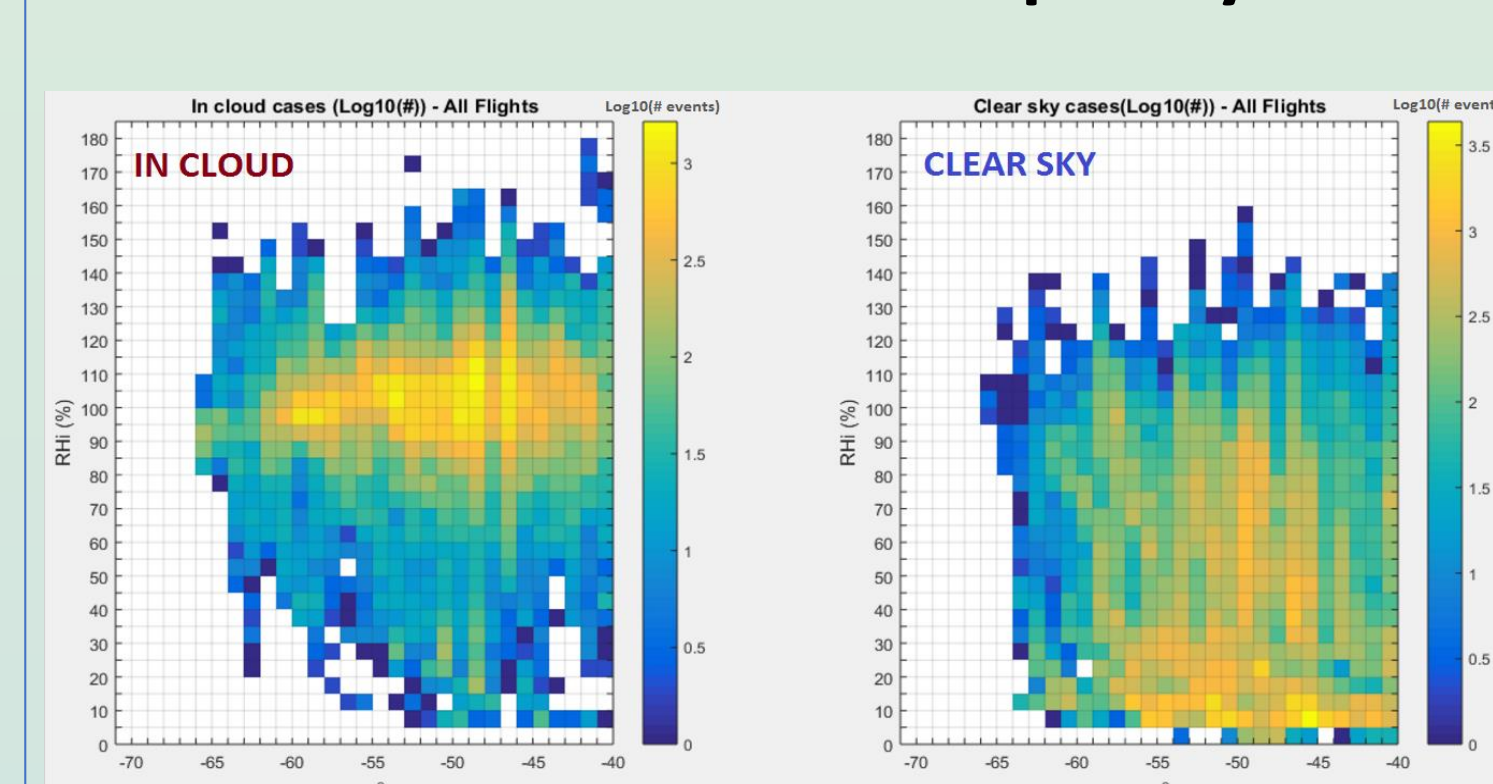
One second merged data from NCAR's GV aircraft during DC3 is compared with one output time from WRF in a region penetrated by GV on May 19th, 2012 at 20:00:00 UTC (As shown on the right). The following methodology compares all GV flight observations to grid points from WRF for two microphysics schemes: Thompson (2009) and Morrison (2008) via statistical analyses.



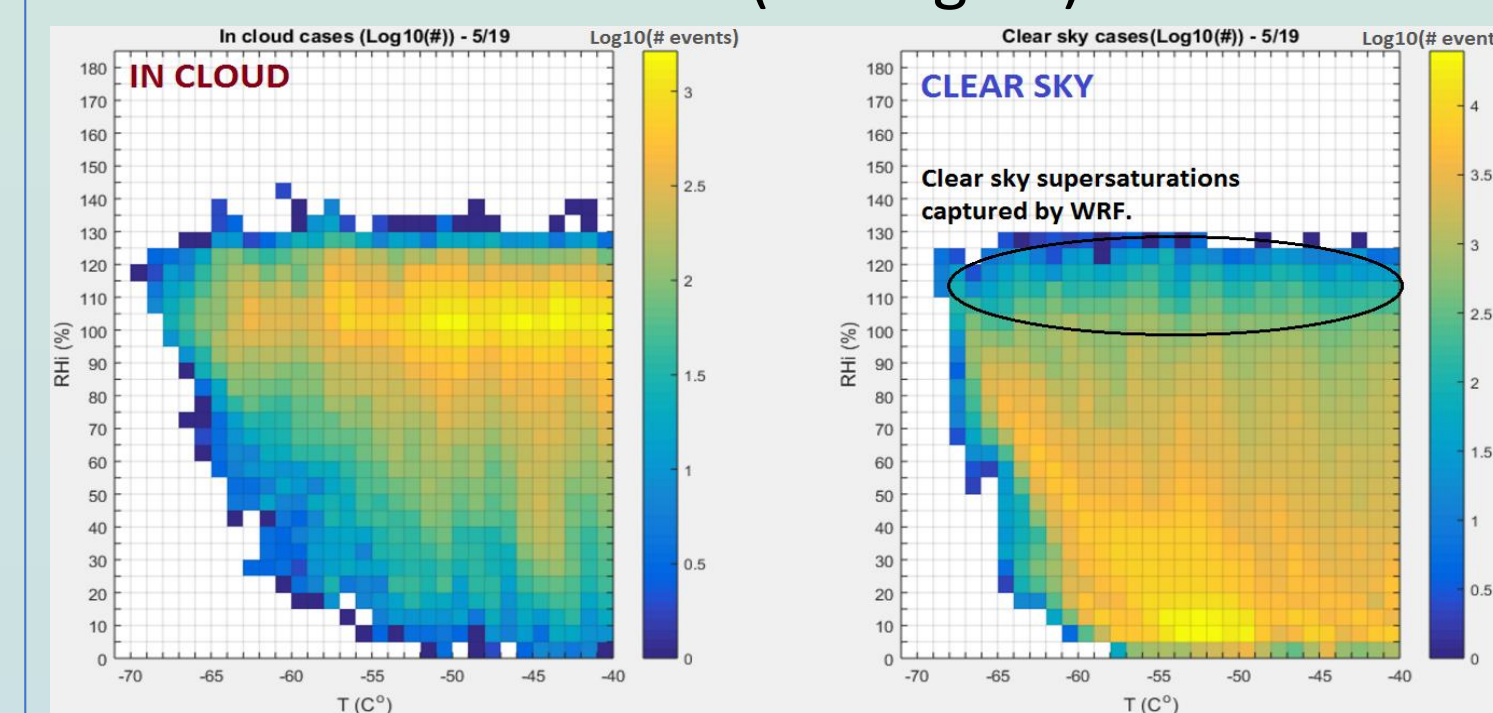
*WRF Resolutions - Coarse: 384x251x40, Nested: 700x580x40 (above)

Conditions required for either using the data point or for determining in cloud vs clear sky observations:
Temperature: All data must be $\leq -40^{\circ}C$. This assures all cloud particles are in the ice phase and no mixed cloud conditions are considered
Vertical Velocity: Measure of updrafts and downdrafts. Due to turbulence associated with convection, airborne obs. rarely exceed updrafts $> 4 \text{ ms}^{-1}$.
Pressure – Restricts observations to upper troposphere, in order to prevent stratospheric observations/associated dry air intrusions.
Ice Water Content (IWC) – A minimum IWC threshold is set for designating in cloud data for consistency between airborne observations and WRF output.

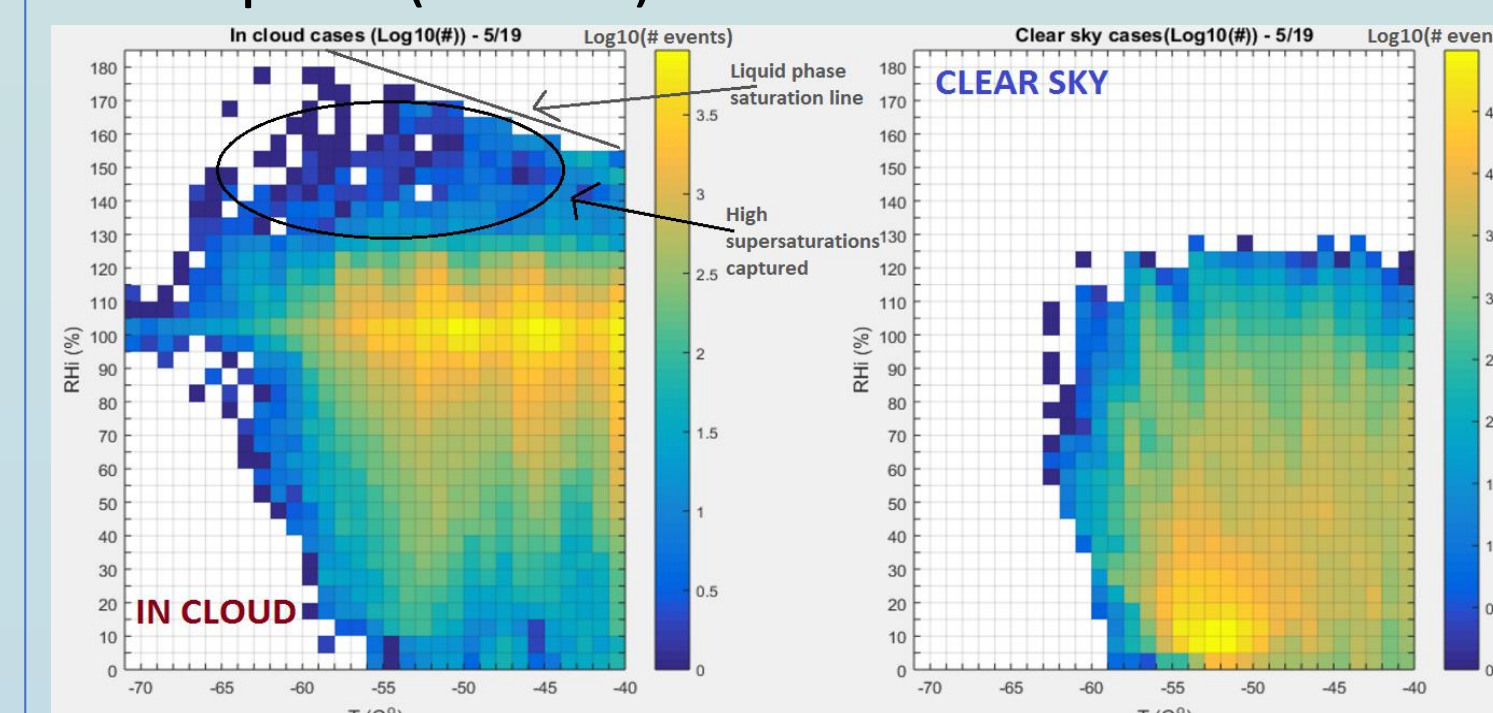
1. RHI Occurrence Frequency



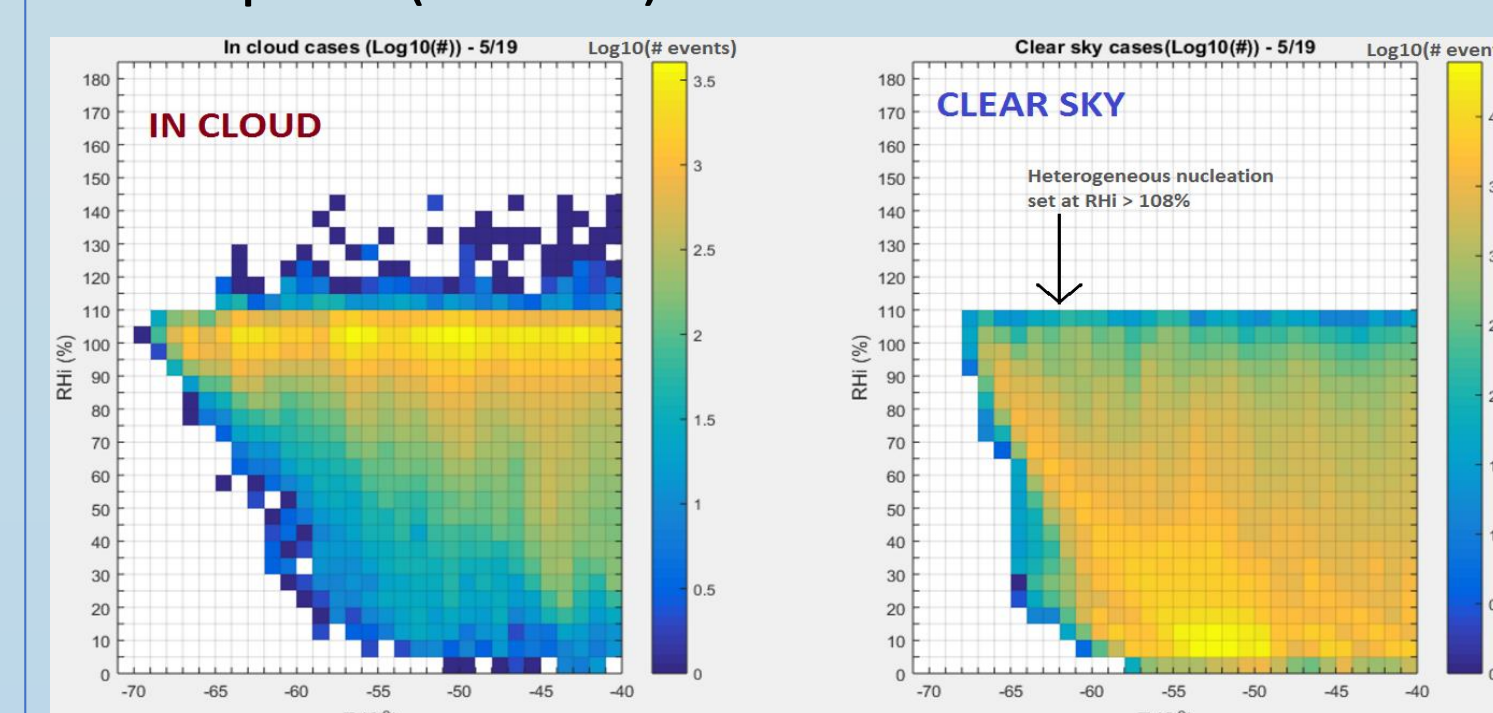
DC3 Observations: GV (All Flights)



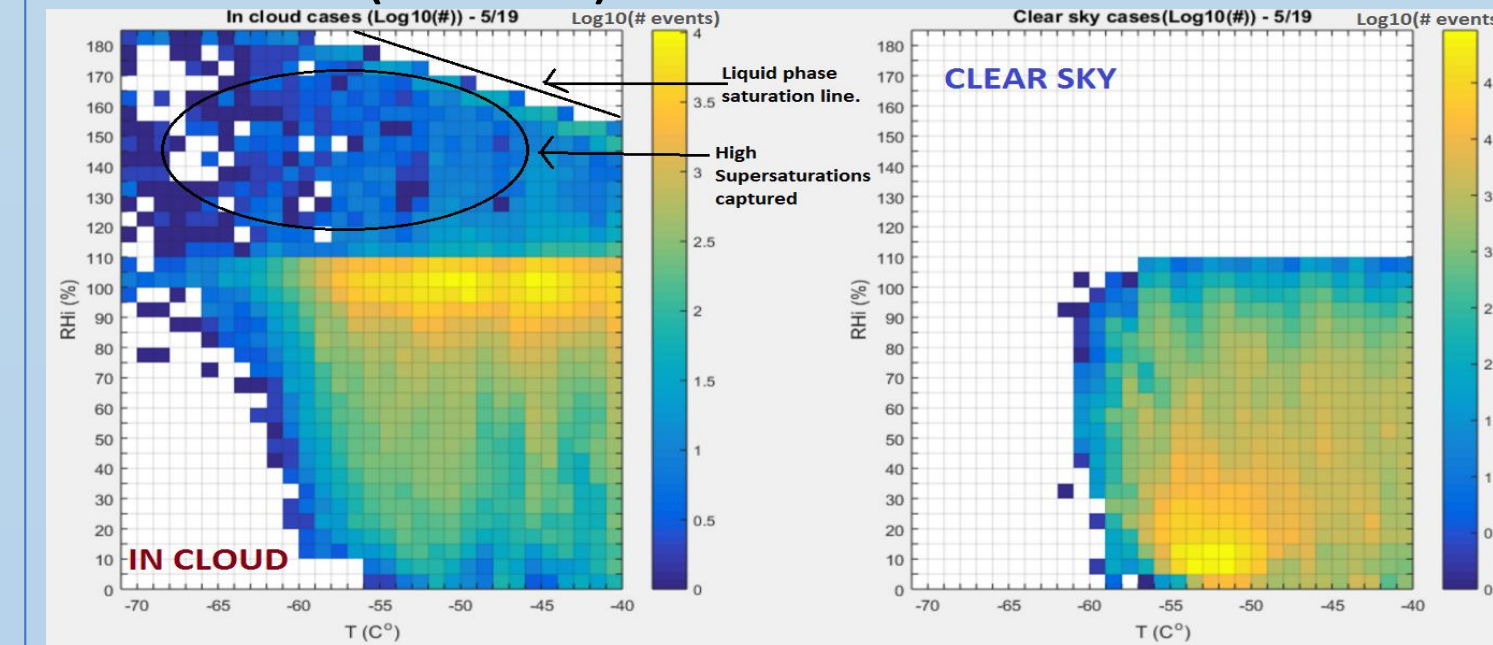
Thompson (Coarse)



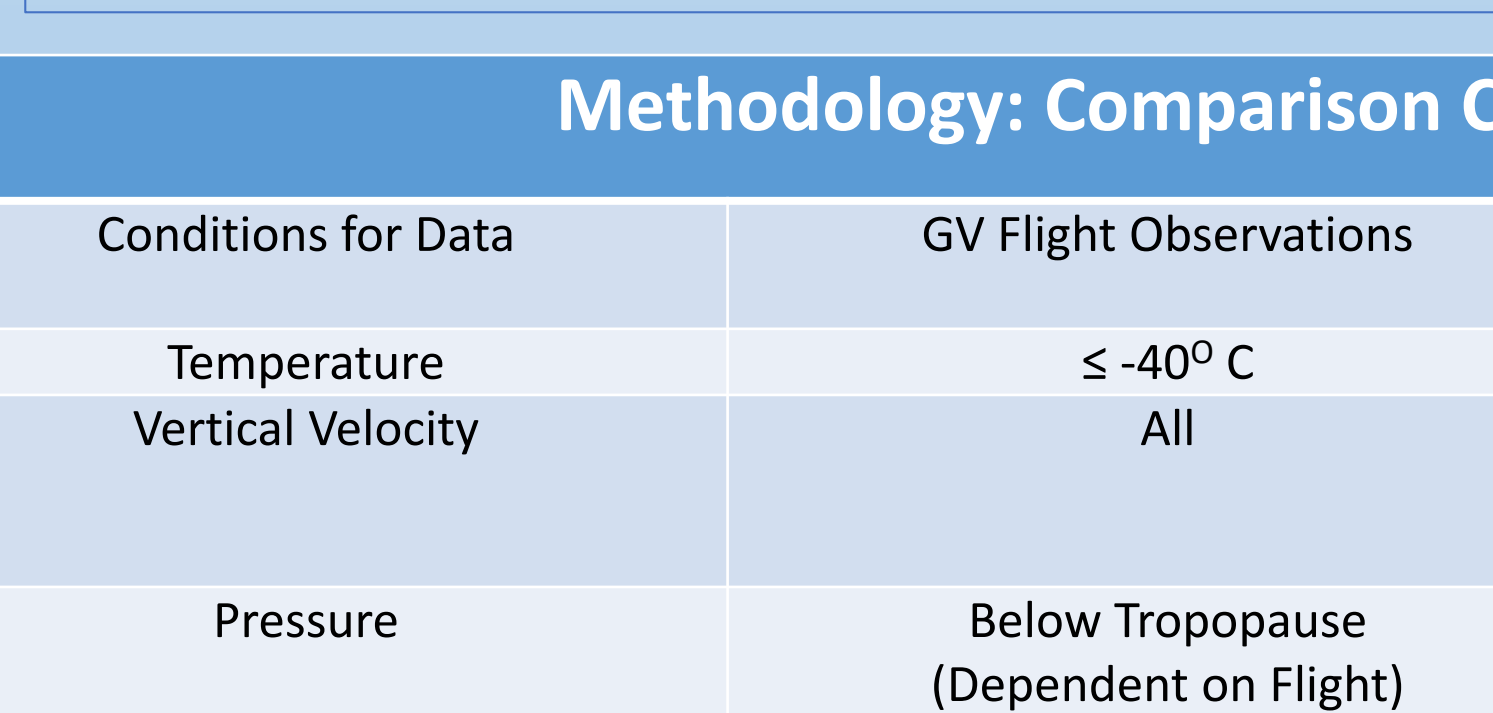
Thompson (Nested)



Morrison (Coarse)



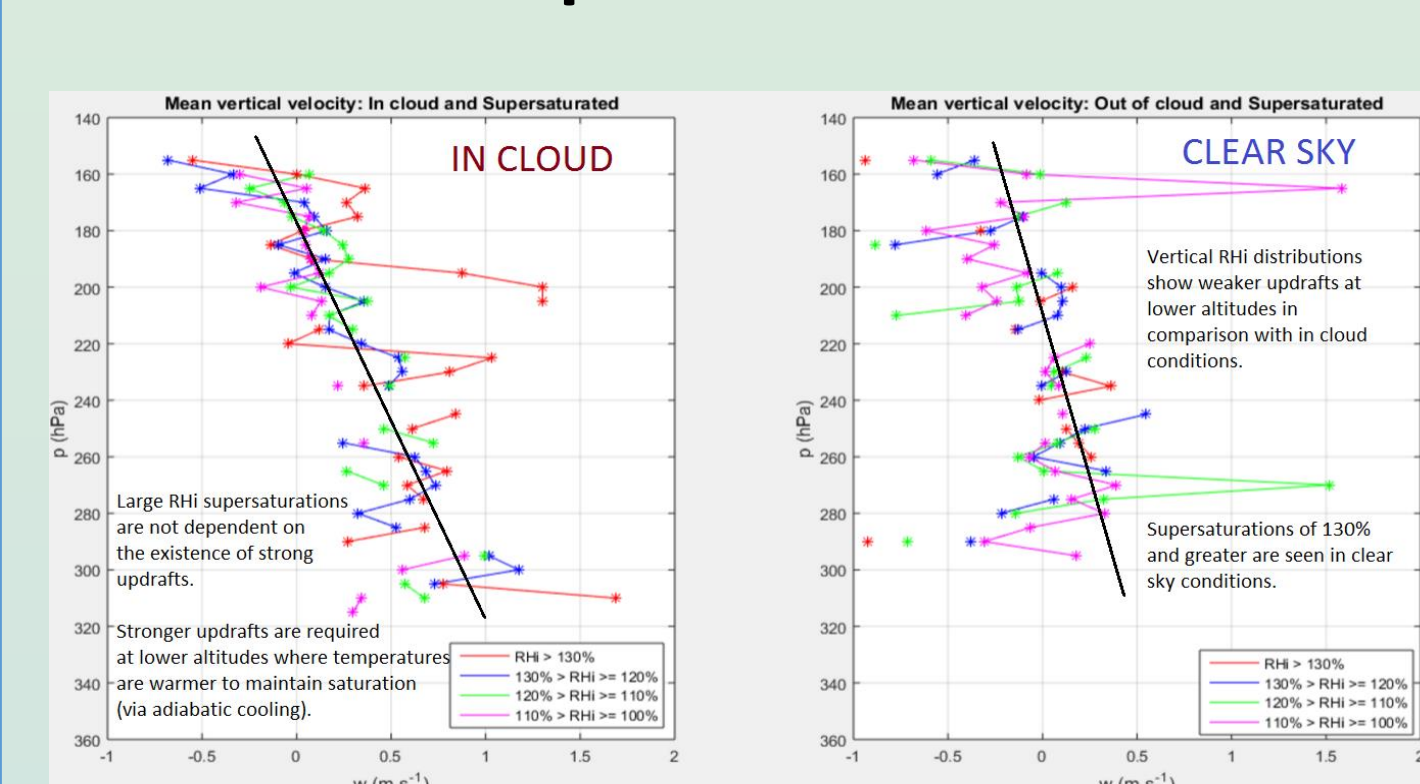
Morrison (Nested)



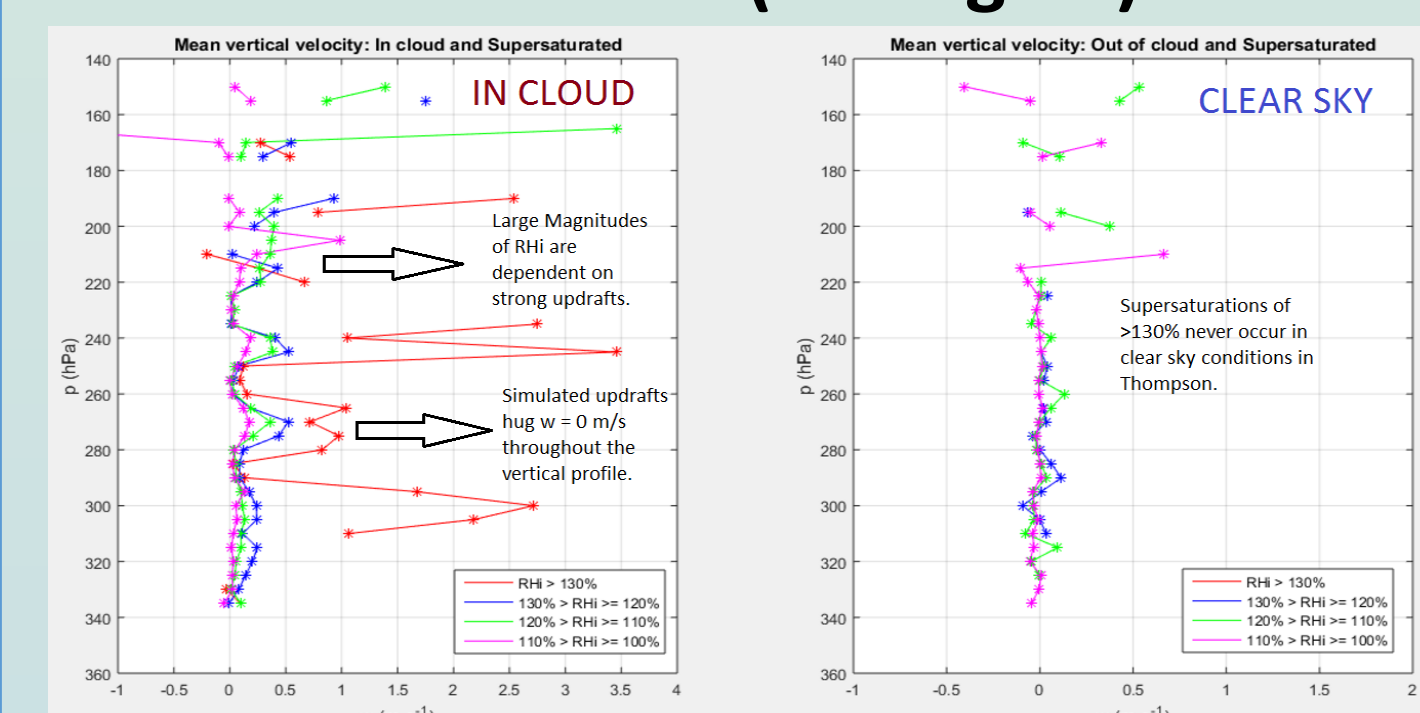
Methodology: Comparison Conditions			
Conditions for Data	GV Flight Observations	WRF Grid Points	
Temperature	$\leq -40^{\circ}C$	$\leq -40^{\circ}C$	
Vertical Velocity	All	All (except for cumulative frequency distributions, p vs mean w, and linear regression/standard error $\sim < -4 \text{ m s}^{-1}$)	
Pressure	Below Tropopause (Dependent on Flight)	$\geq 147 \text{ hPa}$ (Lowest pressure detected in DC3 by GV on May 19 th , 2012)	
Ice Water Content (IWC)	$> 0 \text{ g m}^{-3}$	$\geq 3.8157 \text{ g m}^{-3}$ (Lowest IWC detected in DC3 by GV)	

Measurements	Instrument	Accuracy	Precision
Temperature	Rosemount Temperature Probe	$\pm 0.5 \text{ K}$	$\pm 0.01 \text{ K}$
Vertical Velocity	Radome Gust Wind Package	0.1 m s^{-1}	0.012 m s^{-1}
Ice water content (IWC)	2DC Ice Probe	Ice crystal diameter: 25 – 1600 μm (Korolev et al., 2011) (Only analyze $> 75 \mu\text{m}$)	
Water vapor	VCSEL Hygrometer (Zondlo et al., 2010)	$\pm 6\%$	$\pm 1\%$

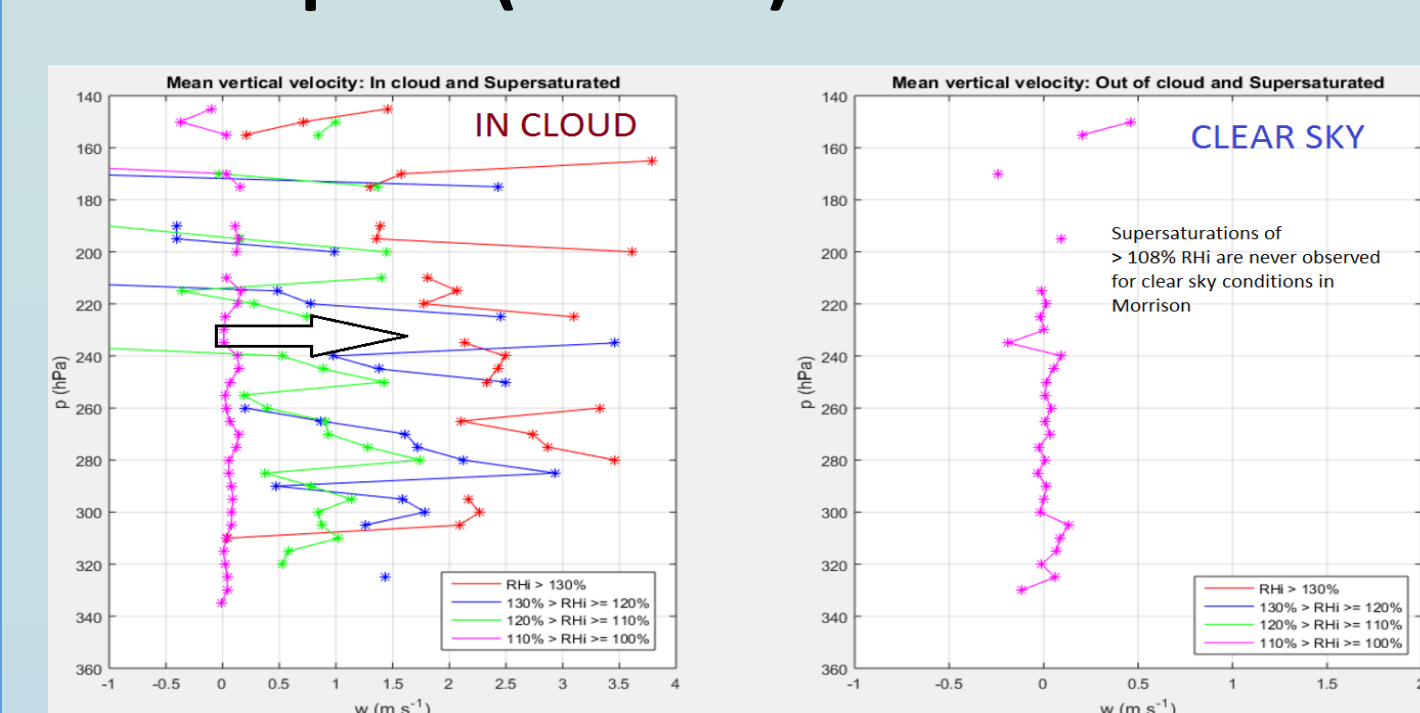
2. Vertical RHI profiles related to w.



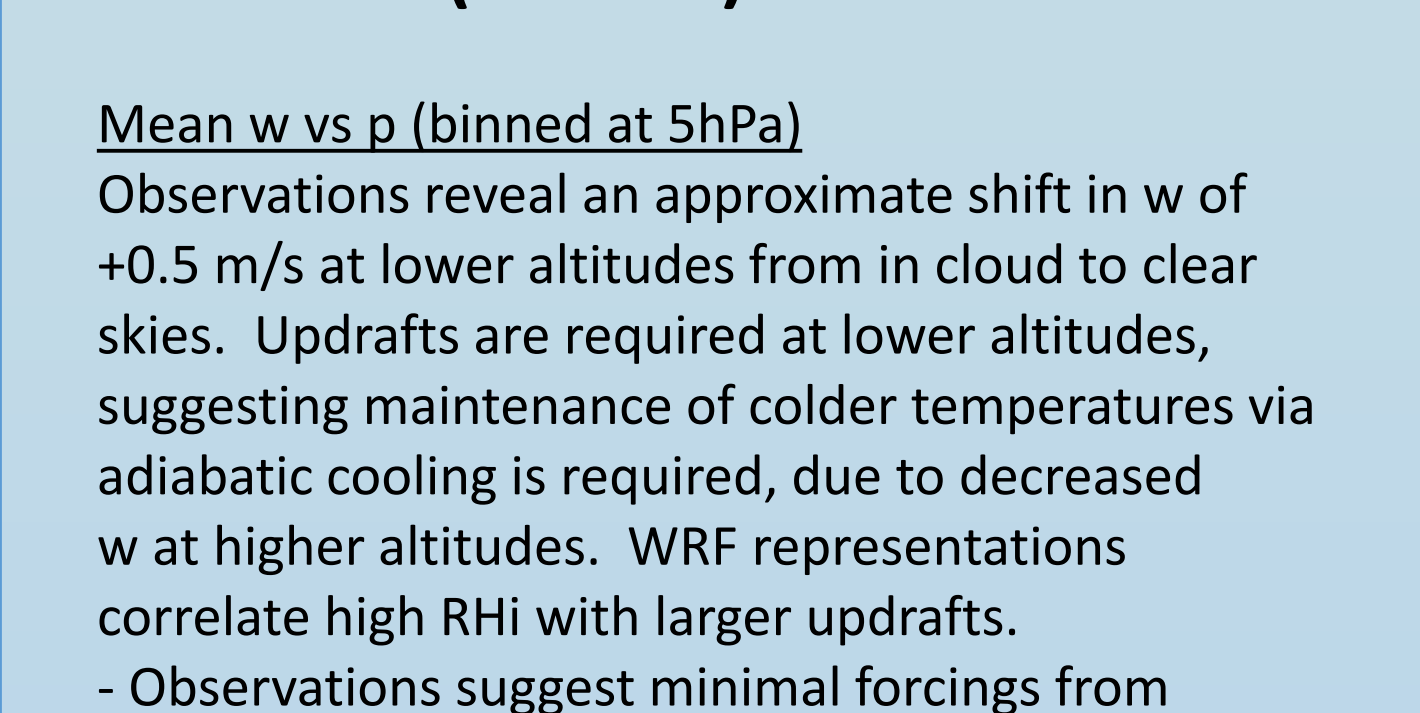
DC3 Observations (All Flights)



Thompson (Nested)



Morrison (Nested)

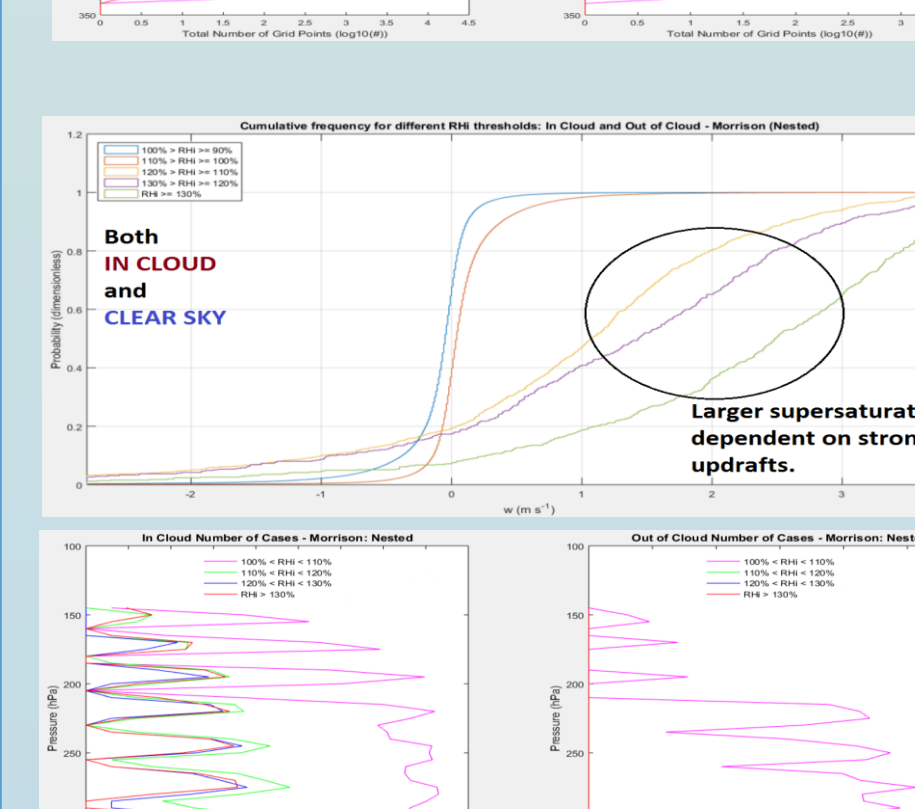
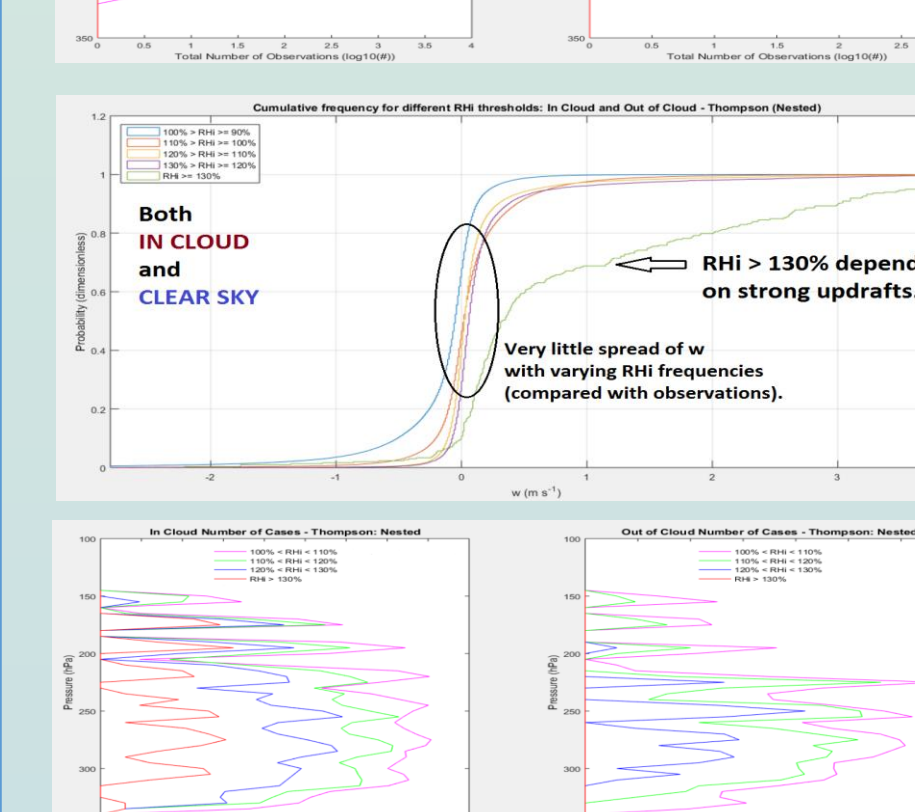
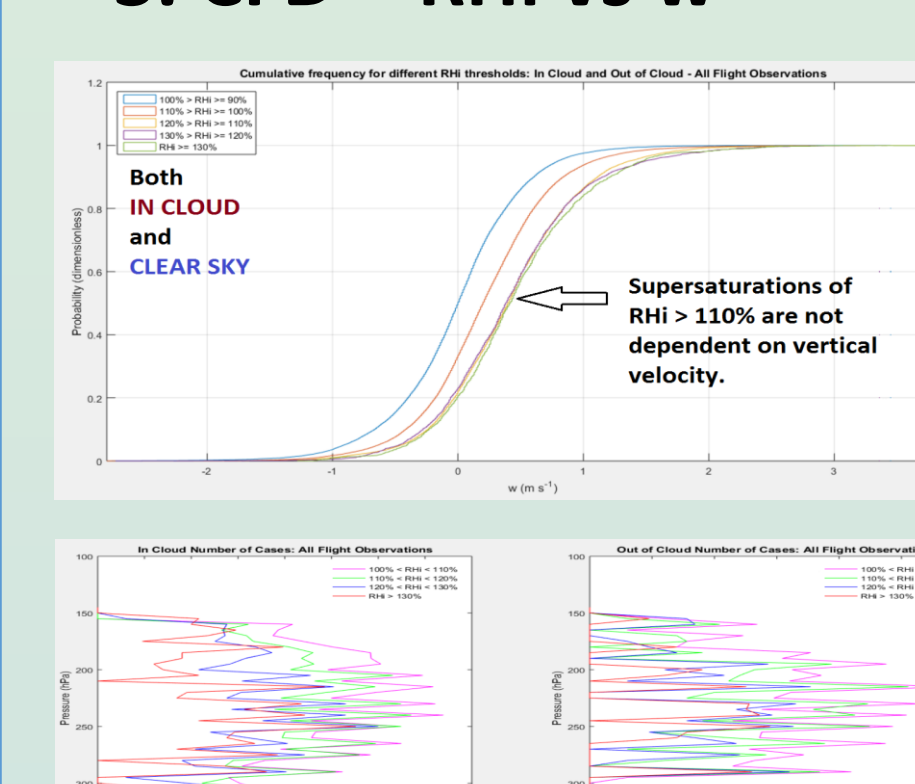


Mean w vs p (binned at 5hPa)
Observations reveal an approximate shift in w of $+0.5 \text{ m/s}$ at lower altitudes from in cloud to clear skies. Updrafts are required at lower altitudes, suggesting maintenance of colder temperatures via adiabatic cooling is required, due to decreased w at higher altitudes. WRF representations correlate high RHI with larger updrafts. - Observations suggest minimal forcings from updrafts are required to sustain high RHI, this provides observational evidence for Kramer et al. (2015) simulation studies which suggest high vertical updrafts will initiate nucleation and then rapidly deplete the water vapor, due to the quick production of high IWC contents/thick ice clouds^(d).

RHI Occurrence Frequency: In cloud vs. clear sky:

Both Thompson and Morrison schemes in WRF capture ISS tendencies for in cloud and out of cloud regions similar to observations. This is a major improvement compared to the CM1 comparisons of an idealized squall line, where the max occurrence frequency of in cloud ISS is below 100% RHI.

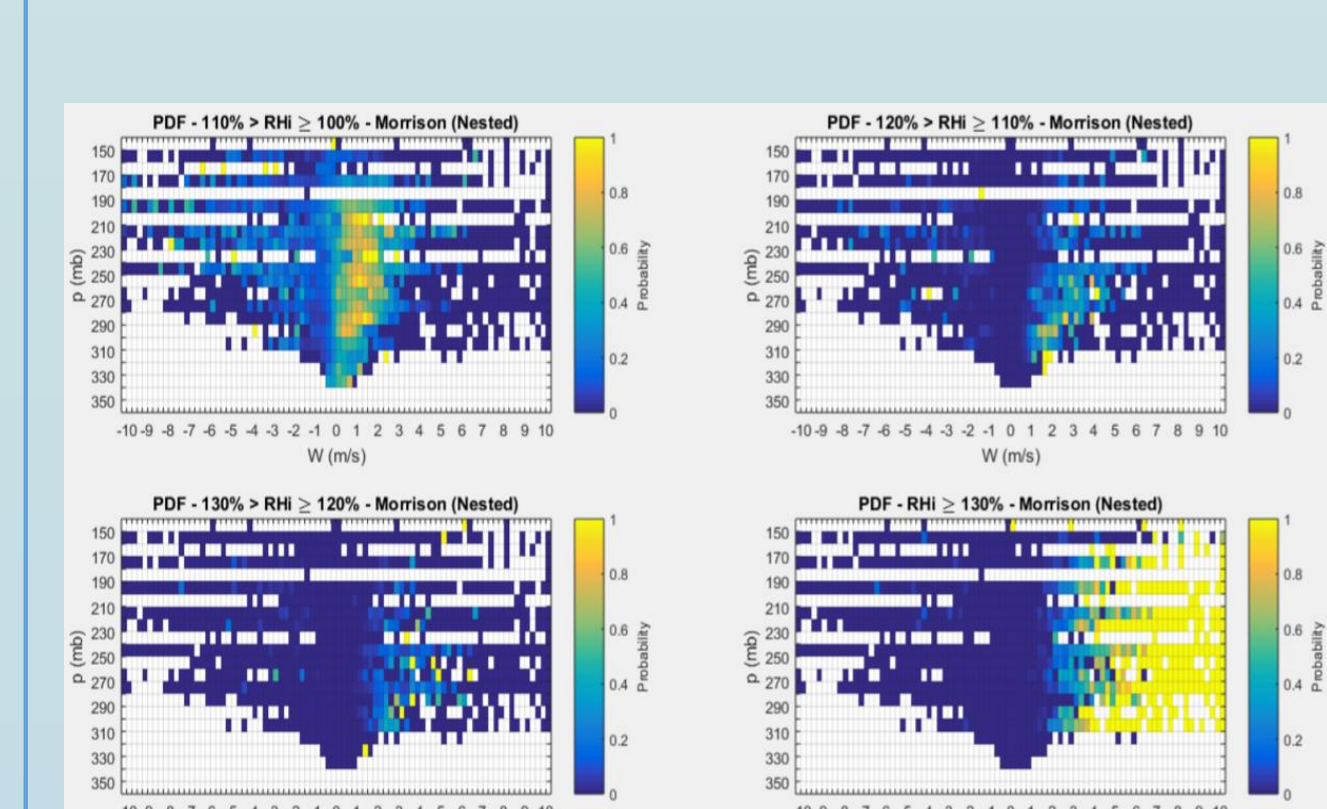
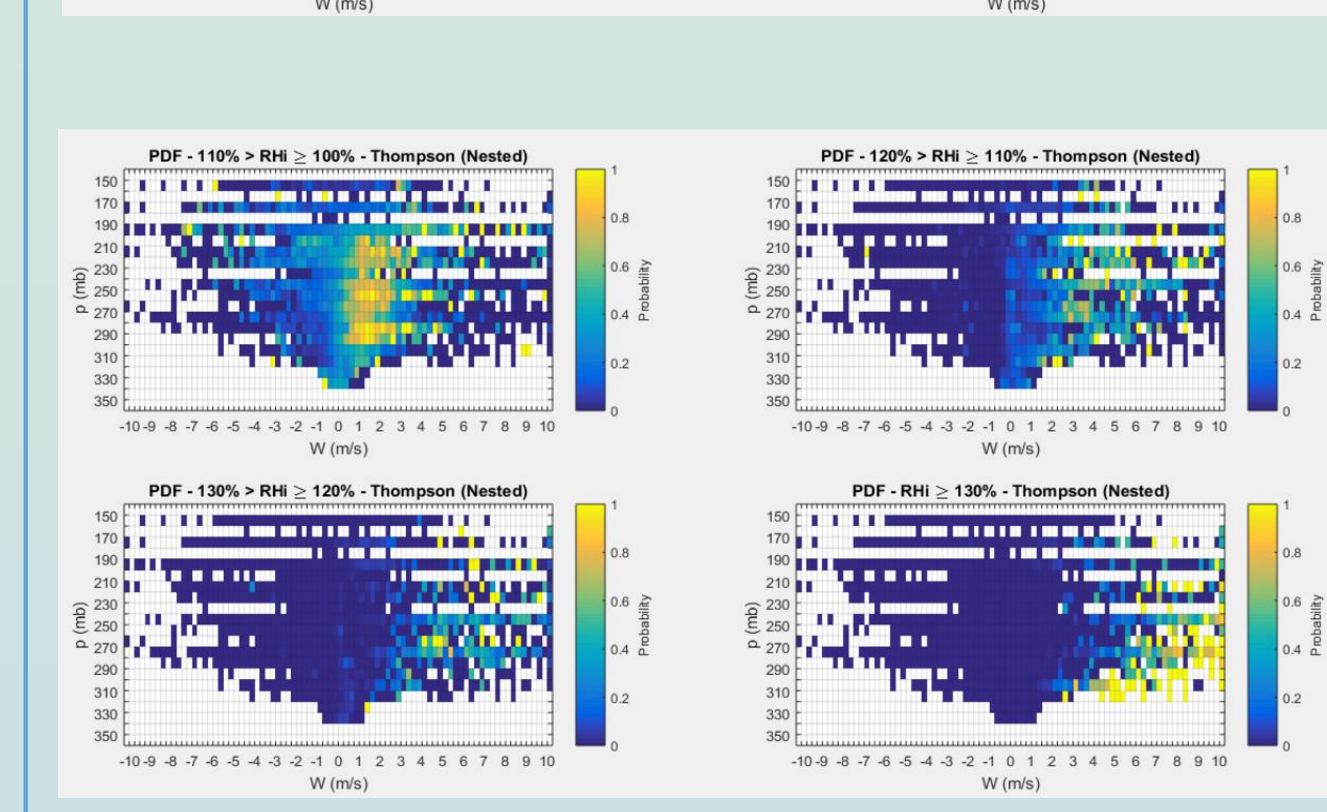
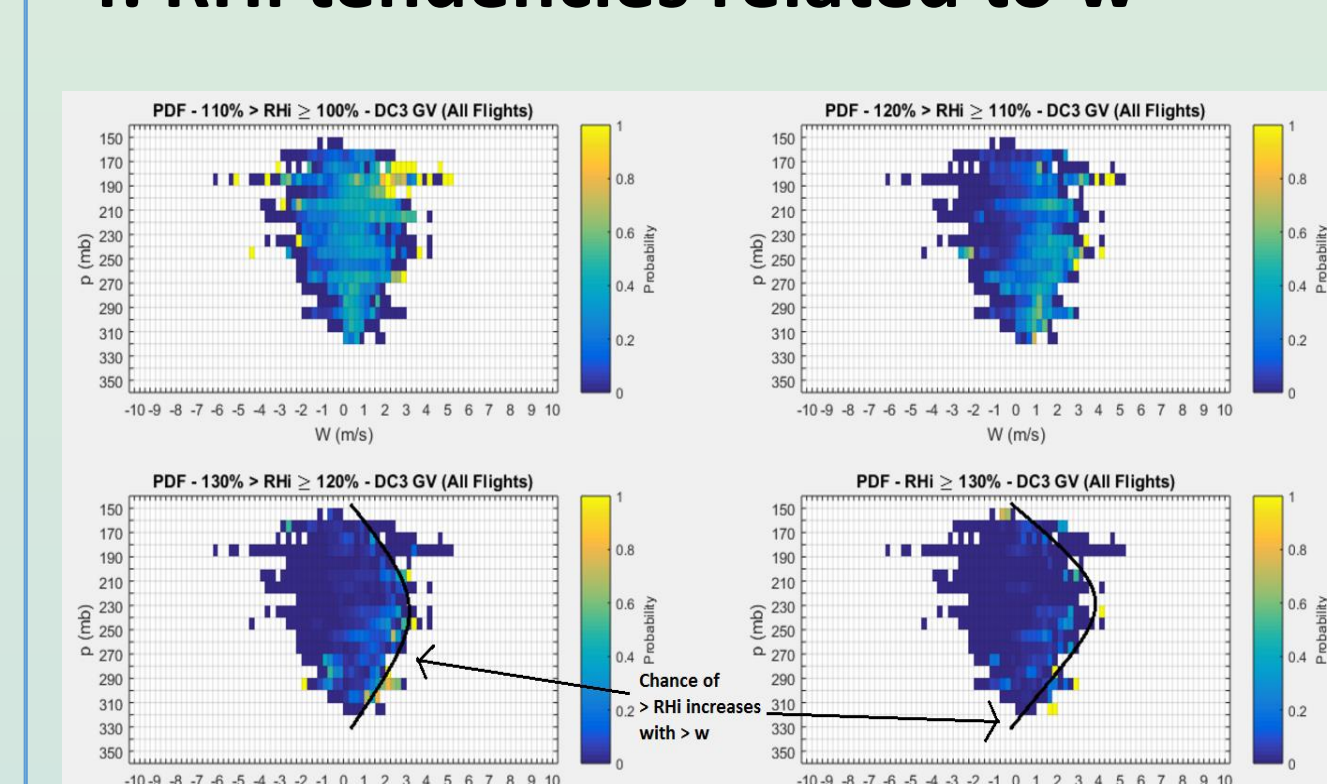
3. CFD – RHI vs w



Cumulative Distribution Frequency (CDF) of both in cloud and clear sky
- Stronger updrafts correspond to high RHI, however, forcings from w are minimal for high supersaturations (RHI $\geq 110\%$)
- RHI in WRF is very sensitive to w forcings near 0 m s^{-1} .
- WRF does not capture gradual decrease of RHI with increasing w as seen in observations.

Total # Observations/Grid Points for Mean w vs p (bottom)

4. RHI tendencies related to w



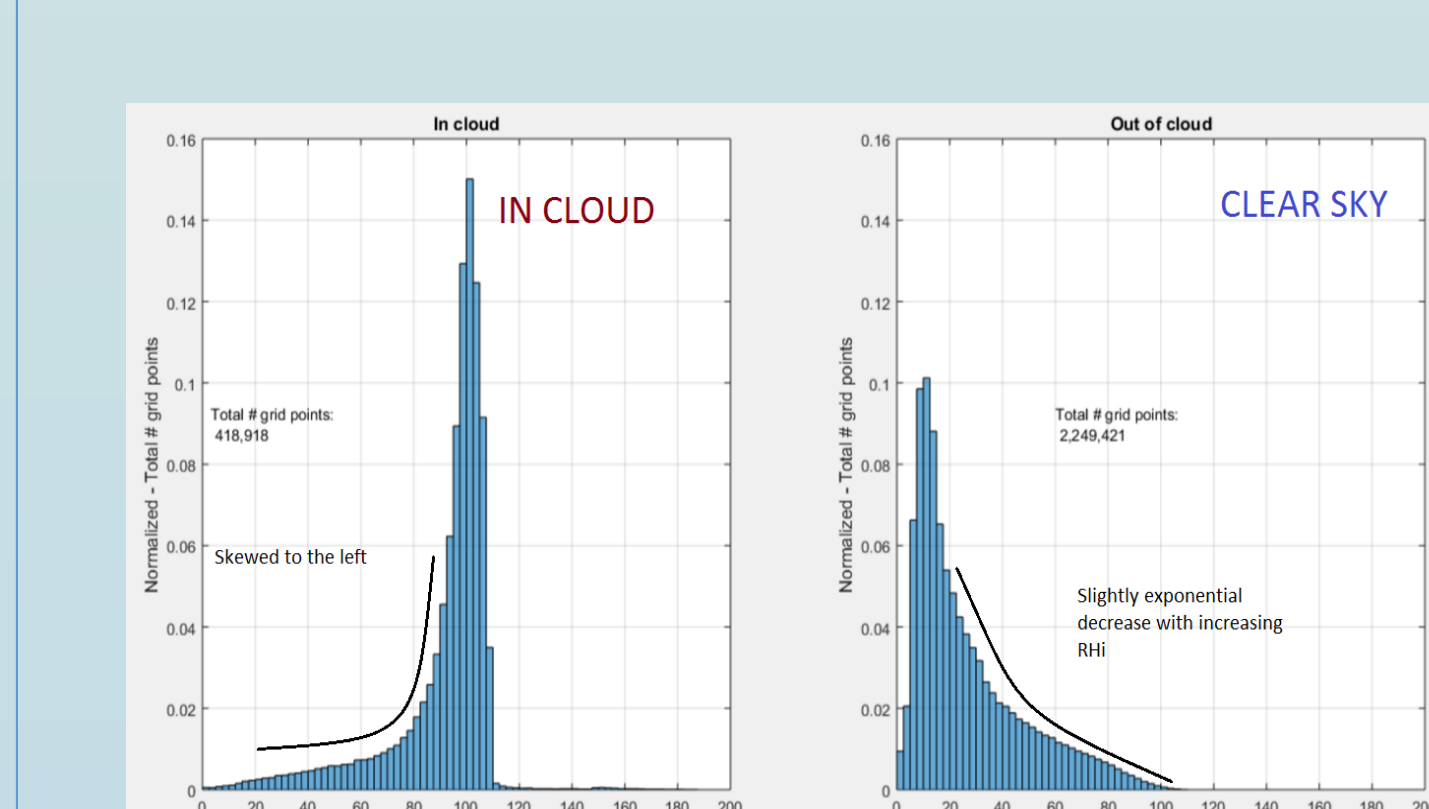
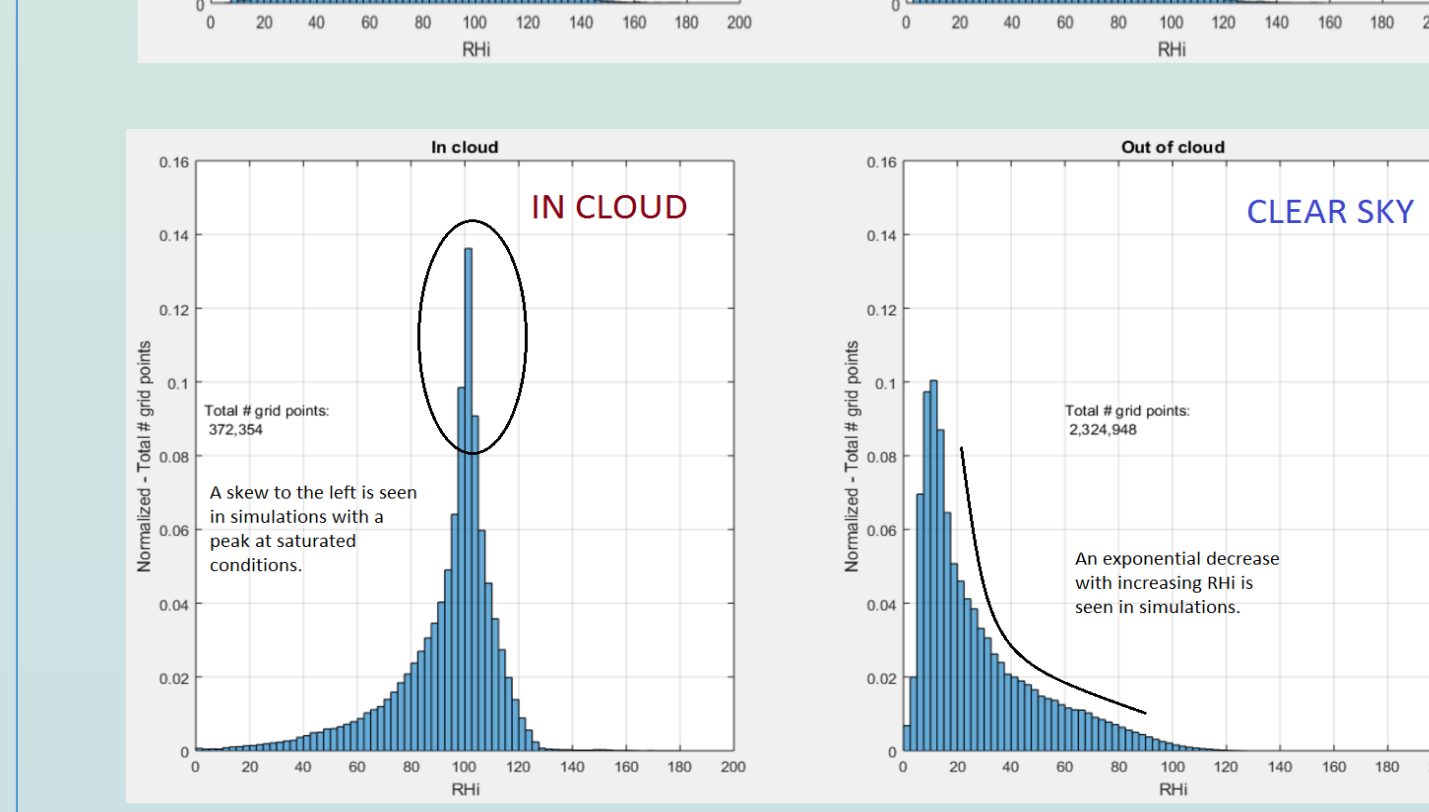
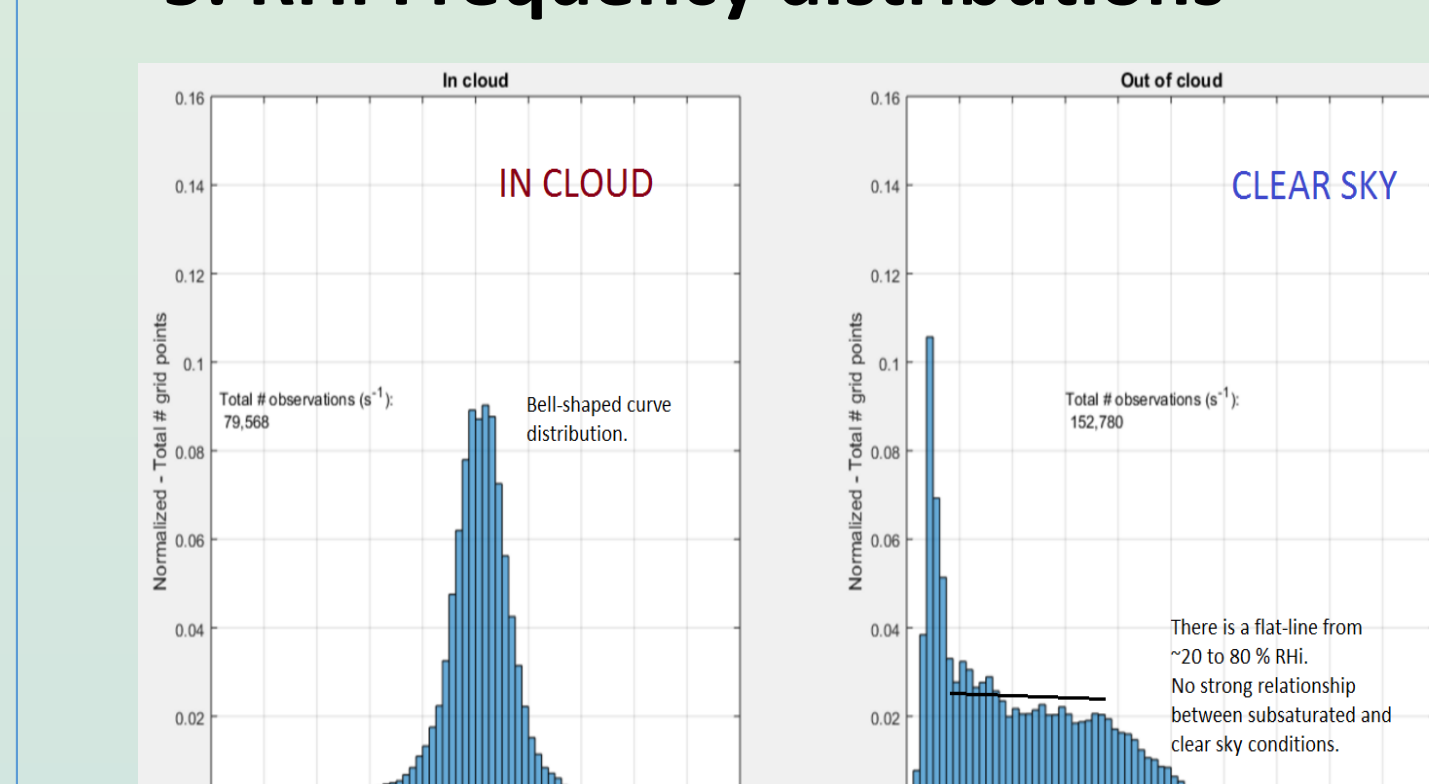
PDFs for varying RHI thresholds (In Cloud) – WRF tends to increase RHI as a function of updraft magnitudes. Observations suggest strong updrafts are not required for higher RHI. However, stronger updrafts at lower altitudes suggest updrafts, which can be minimal, are favorable for high RHI. This confirms a dependency on w for simulations accounting for all w magnitudes in simulations.

Conclusions: Both Thompson and Morrison Capture realistic ISSR frequencies for in cloud and clear sky conditions.

Findings strongly suggest that strong updrafts are not required to reach high supersaturations. This is consistent with Diao et al. (2014) that the primary factor for supersaturations formed in nature is the spatial heterogeneities of water vapor and not the spatial heterogeneities of temperature (via vertical velocity fluctuation).

References:
(a) Diao, M., G. Bryan, H. Morrison, J.B. Jensen, Sensitivity of ice supersaturated region's characteristics to spatial resolution in an idealized squall line scenario, in preparation.
(b) Diao, M., M.A. Zondlo, A.J. Heymsfield, L.M. Avallone, M.E. Paige, S.P. Beaton, T. Campos and D.C. Rogers. 2014: "Cloud-scale ice supersaturated regions spatially correlate with high water vapor heterogeneities", Atmospheric Chemistry and Physics, 14, 2639-2656.
(c) Andrew J. Heymsfield, Larry M. Miloshevich, Carl Schmitt, Aaron Bansemmer, Cynthia Twohy, Michael R. Poellot, Ann Fridlind, and Hermann Gerber. 2005: Homogeneous ice nucleation in subtropical and tropical convection and its influence on cirrus anvil microphysics. J. Atmos. Sci., 62, 41–64
(d) Kramer, M., C. Rolf, A. Luebke, A. Achine, N. Spelten, A. Costa, M. Zoger, J. Smith, R. Herman, B. Buchholz, V. Ebert, D. Baumgardner, S. Borrmann, M. Klingebiel, and L. Avallone. 2015: A microphysics guide to cirrus clouds – Part 1: Cirrus types. Atmos. Chem. Phys., 15, 31537-31586
(e) Murphy, D. M., and T. Koop. 2005: Review of the vapor pressures of ice and supercooled water for atmospheric applications. Q. J. R. Meteorol. Soc., 131, 1539-1565.

5. RHI Frequency distributions



In cloud and Out of cloud Histogram:
In cloud GV observations exhibit a well rounded bell curve, while WRF in cloud gridded regions are skewed to the left (towards decreasing RHI)
- Initiating the production of ice in WRF appears to be very sensitive to RHI (IWC is not accounted for, rate of vapor depletion is another factor). ISSRs are not as prevalent as in GV observations.
- Out of cloud GV observations have a steady frequency of RHI between ~20% to ~80%. WRF out of cloud frequencies exponentially decrease with increasing RHI.

Correlations Between w and RHI magnitude for in cloud and clear sky conditions: Linear Regression and Standard Error								
Analysis Type	In cloud: RHI $\geq 130\%$	In cloud: 130% \geq RHI $\geq 120\%$	In cloud: 120% \geq RHI $\geq 110\%$	In cloud: 110% \geq RHI $\geq 100\%$	Clear sky: RHI $\geq 130\%$	Clear sky: 130% \geq RHI $\geq 120\%$	Clear sky: 120% \geq RHI $\geq 110\%$	Clear sky: 110% \geq RHI $\geq 100\%$
DC3 GV (All flights)	Linear Regression: $w = 0.0056537^*p - 0.77$	Linear Regression: $w = 0.007937^*p - 1.51$	Linear Regression: $w = 0.0054158^*p - 0.90$	Linear Regression: $w = 0.0044505^*p - 0.85$	Linear Regression: $w = 0.0027409^*p - 0.67$	Linear Regression: $w = 0.0032235^*p - 0.77$	Linear Regression: $w = 0.0038294^*p - 0.91$	Linear Regression: $w = 0.0016469^*p - 1.40$
Thompson (Nested)	Linear Regression: $w = -2.2234e-5^*p + 0.96$	Linear Regression: $w = -0.0035362^*p + 1.19$	Linear Regression: $w = -0.0056684^*p + 1.73$	Linear Regression: $w = 0.00098725^*p - 0.21$	N.A.	Linear Regression: $w = 0.00021475^*p - 0.05$	Linear Regression: $w = -0.0018177^*p + 0.52$	Linear Regression: $w = -0.00021182^*p + 0.06$
Morrison (Nested)	Linear Regression: $w = 0.0049527^*p + 0.96$	Linear Regression: $w = 0.012388^*p + 1.98$	Linear Regression: $w = 0.0039601^*p + 0.41$	Linear Regression: $w = 0.0022139^*p - 0.57$	N.A.	N.A.	N.A.	Linear Regression: $w = -0.00065451^*p + 0.20$
	Standard Error: 0.0480	Standard Error: 0.0400	Standard Error: 0.0358	Standard Error: 0.0427	Standard Error: 0.1237	Standard Error: 0.0474	Standard Error: 0.0367	Standard Error: 0.0345
	Standard Error: 0.2046	Standard Error: 0.0513	Standard Error: 0.0893	Standard Error: 0.0596	Standard Error: N.A.	Standard Error: 0.0749	Standard Error: 0.0998	Standard Error: 0.0624
	Standard Error: 0.1822	Standard Error: 0.258	Standard Error: 0.1524	Standard Error: 0.0708	Standard Error: N.A.	Standard Error: N.A.	Standard Error: N.A.	Standard Error: 0.0792